Molecular and Cellular Biochemistry **272:** 187–199, 2005.

Regulation of Ca^{2+}-induced permeability transition by Bcl-2 is antagonized by Drp1 and hFis1

Dejuan Kong,[1] Liping Xu,[1] Yingjie Yu,[1] Weijia Zhu,[2] David W. Andrews,[2] Yisang Yoon[3] and Tuan H. Kuo[1]

[1]*Department of Pathology, Wayne State University School of Medicine, Detroit, MI, U.S.A.;* [2]*Department of Biochemistry, McMaster University, Hamilton, Ontario, Canada;* [3]*Department of Anesthesiology, and Pharmacology and Physiology, University of Rochester School of Medicine and Dentistry, Rochester, NY, U.S.A.*

Received 7 September 2004; accepted 7 December 2004

Abstract

The regulation of mitochondrial permeability transition (MPT) is essential for cell survival. Un-controlled opening of the MPT pore is often associated with cell death. Anti-death protein Bcl-2 can block MPT as assessed by the enhanced capacity of mitochondria to accumulate and retain Ca^{2+}. We report here that two proteins of the mitochondrial fission machinery, dynamin-related protein (Drp1) and human mitochondrial fission protein (hFis1), have an antagonistic effect on Bcl-2. Drp1, with the assistance of hFis1, sensitizes cells to MPT by reducing the mitochondrial Ca^{2+} retention capacity (CRC). While the reduction of CRC by Drp1/hFis1 is linked to mitochondrial fission, the antagonism between Bcl-2 and Drp1 appears to be mediated by mutually exclusive interactions of the two proteins with hFis1. The complexity of protein–protein interactions demonstrated in the present study suggests that in addition to the previously described role of Bcl-2 in the control of apoptosis, Bcl-2 may also participate directly or indirectly in the regulation of mitochondrial fission. (Mol Cell Biochem **272**: 187–199, 2005)

Key words: mitochondria, permeability transition, Bcl-2, Drp1, hFis1, mitochondrial fission, apotosis, calcium

Abbreviations: Drp1, dynamin-related protein; hFis1, human mitochondrial fission protein; MPT, mitochondrial permeability transition; K38A, dominant negative mutant of Drp1; mFis1, mutant hFis(32-152); OMM, outer mitochondrial membrane; IMM, inner mitochondrial membrane

Introduction

It is now generally accepted that Ca^{2+} can act as either a trigger or modulator of the cell-death process (reviewed in [1]). Altered calcium homeostasis is commonly observed in the endoplasmic reticulum (ER) and mitochondria during either apoptotic or necrotic cell death [1–5]. It has been shown that mitochondrial Ca^{2+} plays an important role in the regulation of death in many cell types including cardiac myocytes and neuronal cells [1, 5]. High concentrations of extracellular Ca^{2+} can lead to mitochondrial Ca^{2+} overload, which in turn activates the mitochondrial permeability transition (MPT), resulting in the loss of matrix Ca^{2+} [5] through "irreversible opening" of the MPT pore. The loss of mitochondrial Ca^{2+} then leads to impaired mitochondrial function and cell death [6–8]. This Ca^{2+}-mediated MPT mechanism involving the inner mitochondrial membrane (IMM) appears to be distinct from the cytochrome *c* release mechanism that

Address for offprints: T.H. Kuo, Department of Pathology, Wayne State University School of Medicine, 540 E. Canfield, Detroit, MI 48201, U.S.A. (E-mail: tkuo@med.wayne.edu)

involves only the outer mitochondrial membrane (OMM) [9–12]. Thus, MPT is an important regulator of mitochondrial-dependent cell death that can involve leakage of both OMM and IMM [13]. Studies with isolated mitochondria indicate that MPT can be induced by the uptake of Ca^{2+} pulses as well as other physiological variables such as pH, magnesium, phosphate, free radicals, adenine nucleotide levels and mitochondrial redox state [14]. A healthy mitochondrion has a defined capacity to accumulate Ca^{2+}, and the anti-death protein Bcl-2 increases the capacity of mitochondria to retain excess Ca^{2+} by blocking opening of the MPT pore [6, 15, 16]. The inhibition of MPT by Bcl-2 is supported by the finding that Bcl-2 also increases the resistance of mitochondria to undergo Ca^{2+}-induced swelling [6]. However, it is not understood how Bcl-2 blocks the MPT during mitochondrial Ca^{2+} overload.

In living cells, mitochondria are dynamic structures that frequently divide and fuse with one another [17]. At least two types of mitochondrial morphology have been observed: a tubular (connected) form and a punctate (disconnected) form [17]. A novel dynamin-related GTPase named dynamin-related protein (Drp1) has been shown to regulate the transition from the tubular form to the punctate form [18–21]. Presumably, Drp1 mediates mitochondrial fission *via* the severing of the mitochondrial outer membrane [22]. Although Drp1 is known to function as a mitochondrial fission enzyme, overexpression of Drp1 in mammalian cells does not change mitochondrial morphology noticeably [19, 22], indicating that there are other limiting factors in the mitochondrial fission process. Overexpression of another factor human mitochondrial fission protein (hFis1) induces mitochondrial fragmentation in a Drp1-dependent manner [23–25]. It has been suggested that hFis1 regulates mitochondrial fission through a protein–protein interaction that recruits Drp1 from the cytoplasm to the mitochondrial surface [23]. The fragmentation of the mitochondrial network into the punctate form has also been observed during cell death induced by various apoptotic stimuli [26]. Despite the importance of Drp1 and hFis1 in the regulation of mitochondrial morphology, whether or not these proteins affect Ca^{2+}-induced MPT remains largely unknown [27]. If these proteins contribute directly or indirectly to the opening of the MPT pore during fission and fusion, it would represent a previously unrecognized potential site of regulation by Bcl-2 family proteins. However, a potential role of Bcl-2 in the regulation of the biological activity of Drp1 and hFis1 during cell survival or death has not been examined.

We report here that deregulation of Drp1 and hFis1 disrupts mitochondrial function as overexpression of either Drp1 or hFis1 reduces the mitochondrial Ca^{2+} retention capacity (CRC). In contrast, overexpression of Bcl-2 increases mitochondrial CRC. The antagonism between Bcl-2 and Drp1 appears to be mediated through competition for binding to hFis1.

Material and methods

Cell culture and transfection procedures

COS epithelial cells were grown in high glucose DMEM (Invitrogen) supplemented with 10% FBS. Stable MCF7 cell lines overexpressing human wild-type Bcl-2 or an empty PrCCMV vector as a control were established as described previously [28] and are referred to here as MCF7 Bcl-2 or MCF7CMV cell line. Transfections were carried out using Lipofectamine 2000 reagent according to manufacturer's protocol (Invitrogen). The ratio of DNA to cationic lipid reagent was kept at 0.4 μg/μl. Under this condition, the efficiency of transfection of a control plasmid expressing green fluorescence protein scored visually by fluorescence microscopy for COS-7, MCF7CMV and MCF7 Bcl-2 cells was 90, 60, and 30%, respectively. Human pcDNA3-Drp1 and the dominant negative mutant pcDNA3-DrpK38A (designated as K38A) were obtained from Dr. A.M. van der Bliek (University of California, Los Angeles). Human Myc-tagged hFis1 in pcDNA3 has been described previously [23]. Transient expression of Drp1 protein, Myc-hFis1 protein, and the K38A mutant were carried out for 24 h, and cells were then used for biochemical assays.

Mitochondrial Ca^{2+} retention assay

Mitochondrial retention of Ca^{2+} was assayed for permeabilized cells as described by Murphy *et al.* [15] using the calcium indicator Calcium Green-5N (Molecular Probes). Briefly, COS-7, MCF7CMV, or MCF7Bcl-2 cells transfected with Drp1, Myc-hFis1, K38A or mutant Myc-hFis1 were harvested by trypsinization followed by centrifugation. The cells (1×10^7 cells/2 ml) were resuspended in respiratory buffer (125 mM KCl, 2 mM K_2HPO_4, 1 mM $MgCl_2$, 20 mM Hepes, pH 7.0) containing 0.1 μM Calcium Green-5N and 5 mM glutamate and 5 mM malate, and the plasma membranes were permeabilized by the addition of digitonin (final concentration 0.01%). Previous control studies had shown that digitonin treatment did not affect the integrity of the mitochondria as determined by assaying oxidative phosphorylation [29, 30]. The respiratory control ratio of the mitochondria remained the same with or without digitonin treatment, except that digitonin treatment gave a better yield of mitochondria [29]. The calcium retention assay began with successive additions of $CaCl_2$ (10 μM or 25 μM) and the fluorescence changes in response to the addition of Ca^{2+} were monitored continuously at 25 °C in a spectrofluorometer (Photon Technology International) with the excitation at 506 nm and

emission at 531 nm. Calibration of the fluorescence signal was achieved by the addition of known amounts of Ca^{2+} to the medium without the cells.

Western blot analysis

Cells were lysed in Buffer A (1% Triton, 0.1% SDS, 50 mM Tris pH 8.0, 150 mM NaCl, and 1 mM each of EDTA, EGTA, PMSF, and Aprotinin (to inhibit protease) and then incubated on ice for 30 min. Cell lysate was cleared by centrifugation at 10, 000 $\times$ g for 10 min. Protein concentration was measured using the Bradford assay (BioRad) and lysate containing 25 μg of protein was boiled in sample buffer and separated by SDS-PAGE prior to immunoblotting as described previously [31]. The following antibodies were used: Drp1 from BD Transduction Laboratories, Bcl-2 (N-terminal epitope) from Dako, Bcl-2 (aa49-179 epitope) from eBiosciences, hFis1 from Yoon *et al*. [23], Myc from Zymed Laboratories or from Upstate Biotechnologies Inc. The antibody for glyceraldehyde-3- phosphate dehydrogenase (GAPDH) was purchased from Research Diagonostic Inc.

Immunoprecipitation

Cells were harvested and incubated in lysis buffer A (see previous sections) for 30 min on ice. The lysates (250 μg protein per IP) were pre-cleared by incubation with 25 μl Protein G agarose and control IgG (2 μg, Sigma) for 1 h to remove non-specific binding. The lysates were then incubated with the primary antibody overnight at 4 °C, 10 μl Protein G agarose was added and the samples were incubated for 1 h. The Protein G agarose was collected by centrifugation, washed and then boiled in sample buffer. The precipitated proteins were separated by SDS-PAGE and identified by immunoblotting.

Mitochondrial morphology and cell death assay

Cells were grown on coverslips and fixed in 4% *para*-formaldehyde for immunostaining, according to the procedure of Zhu *et al*. [32]. Twenty-four hours after transfection with DNA encoding Myc-hFis1 or mutant Myc-hFis1 (Myc-mFis1), samples were stained with mouse anti-mitochondrial heat shock protein 70 antibodies (HSP70 (1:50), Affinity BioReagents) and Alexa 594 (red) conjugated goat-anti mouse antibody. Double staining was carried out with Myc antibody conjugated to Alexa 488 (green) using Zenon mouse IgG labeling kit (Molecular Probes). Images were obtained using a Leica DML fluorescence microscope. Cell death was also assayed after Myc-hFis1 transfection by counting at least 400 cells and determining the fraction unable to exclude Trypan blue dye. Cell death induced by hFis1 was corrected for spontaneous cell death in controls. In addition to Trypan blue staining, cell death was also determined by counting apoptotic nuclei after staining with Hoechst dye as described previously [16].

Densitometry and data analysis

Protein bands were scanned and the optical density of the bands quantified using the NIH image 1.61 software. Data (mean $\pm$ S.D.) were analyzed by Student's t-test and significance defined as a p-value of <0.05.

Results

Calcium retention capacity in permeabilized cells

Our previous studies in cultured cells [5, 16] and transgenic mice [6] have suggested that the ability of mitochondria to sequester and retain calcium is important for cell survival. However, too much calcium can lead to MPT and cell death [7]. The increased capacity for calcium retention without triggering MPT in Bcl-2 expressing cells indicates increased stability of the IMM due to Bcl-2 expression [6, 15, 16]. We have used a permeabilized cell system to measure Ca^{2+} uptake into mitochondria. The validity of this method in the quantitative analysis of Ca^{2+} sequestration by mitochondria has been described in detail by Murphy *et al*. [15]. Similar results were obtained with either isolated mitochondria or permeabilized cells [15, 30].

Permeabilized COS cells under conditions of mitochondrial respiration (energized with glutamate plus malate) in the presence of phosphate, were able to take up and retain a series of Ca^{2+} pulses at 2 min intervals (Fig. 1A). The accumulation of Ca^{2+} continued until the load reached a threshold of 125 μM (five pulses of 25 μM), at which point the mitochondria underwent a fast process of Ca^{2+} release. The Ca^{2+} threshold for COS cells remained the same when the size of the Ca^{2+} pulses was varied such that on average 12.5 pulses of 10 μM were required to cause the release of Ca^{2+} (data not shown). Similar to previous observations with the isolated mitochondria [6], the precipitous Ca^{2+} release was due to the activation of MPT, because the critical threshold for Ca^{2+} release was increased by the permeability pore inhibitor cyclosporine A (CSA). Figure 1B shows that pre-incubation of COS cells with 0.5 μM CSA for 3 min was sufficient to increase the Ca^{2+} threshold to 250 μM (10 pulses of Ca^{2+}, 25 μM per pulse) confirming the assay measures the Ca^{2+} threshold for MPT. Furthermore, permeabilized COS cells lost the ability to take up the Ca^{2+} pulses (at 10 μM per pulse) in the presence of mitochondrial respiratory inhibitor, antimycin A (1 μM), confirming that Ca^{2+} uptake requires intact, respiring mitochondria (Fig. 1C). To confirm that the

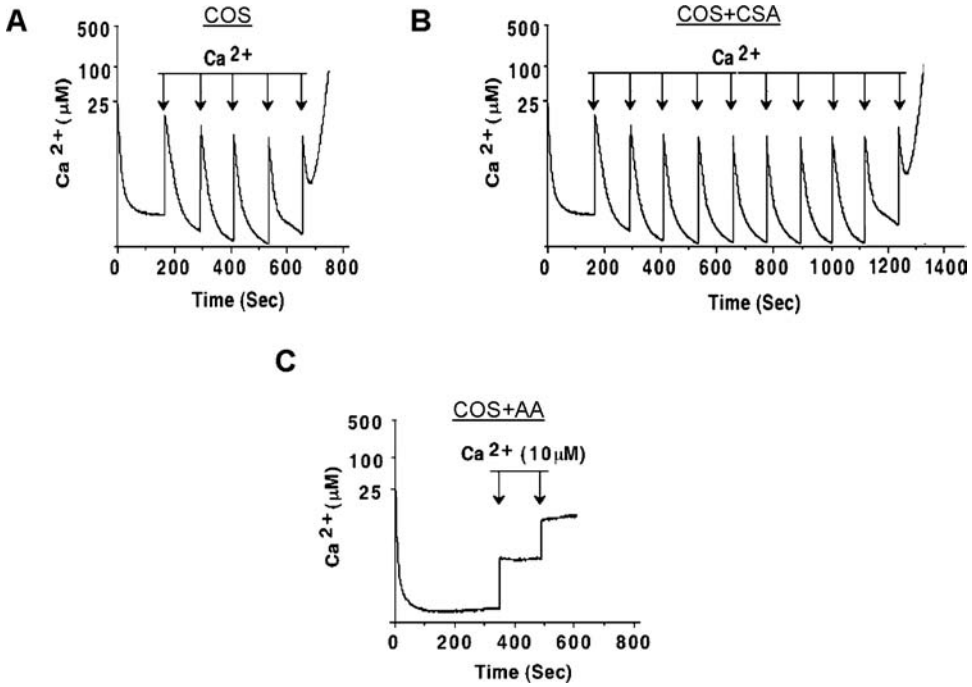

Fig. 1. Assay of Ca^{2+}-induced permeability transition. (A) COS cells (1×10^7) were permeabilized with digitonin (0.01%) and Ca^{2+} uptake was measured by successive additions of 25 μM Ca^{2+} pulses. (B) COS cells were pretreated with cyclosporin A (0.5 μM) for 3 min and Ca^{2+} uptake was measured as mentioned in (A). (C) Ca^{2+} uptake was measured as in (A) except the medium contained the respiratory inhibitor antimycin A (1 μM), and 10 μM (instead of 25 μM) Ca^{2+} pulses were added. Results are typical of three independent experiments.

endoplasmic reticulum does not contribute to Ca^{2+} uptake in digitonin-treated cells, the experiment was conducted in the presence of thapsigargin, a specific inhibitor of the endoplasmic reticulum calcium pump (SERCA). As expected, the Ca^{2+} threshold remained the same with or without the addition of thapsigargin (1 μM) (data not shown) demonstrating that Ca^{2+} uptake by the endoplasmic reticulum was not contributing to Ca^{2+} uptake in permeabilized cells. As previously reported [29, 30], the use of digitonin for cell permeabilization did not affect the respiratory control ratio (or oxidative phosphorylation activity) of the mitochondria. This was further confirmed by the testing of various concentration of digitonin in our assay. We found that the CRC remained the same for digitonin concentrations between 0.05 and 0.2% (data not shown). Thus this assay using permeabilized cells permits quantitative evaluation of the CRC of the mitochondria.

Dynamin-related protein (Drp1) sensitizes mitochondria to calcium-induced permeability transition

COS cells were transfected with Drp1 or empty vector (control) for 24 h, permeabilized and assayed for calcium retention. The results indicated a Ca^{2+} threshold of 125 μM (five pulses of 25 μM Ca^{2+}) for the empty vector transfected controls (Fig. 2A). Transient expression of Drp1 reduced the CRC to 75 μM (or three pulses) (Fig. 2B). Interestingly, the expression of a dominant negative mutant that carries an inactive GTPase domain due to the mutation of lysine 38 to alanine (designated as K38A) was unable to reduce the Ca^{2+} threshold when compared to the control (Fig. 2C and 2A). Results from four independent experiments (Fig. 2D) indicated that the CRC was 65 ± 10 μM for cells overexpressing Drp1 compared to 108 ± 14 μM for the controls, representing a 40% reduction ($n = 5$, $p < 0.015$). In contrast, the average load of 101 ± 15 μM for the cells expressing K38A was essentially the same as the controls ($n = 4$, $p > 0.5$). Thus, the reduction of Ca^{2+} threshold for MPT required overexpression of a GTPase active Drp1.

To further elaborate the effect of overexpression of Drp1 on reducing the CRC, COS cells were transfected with increasing amounts of Drp1-cDNA (from 0 to 48 μg). A time-course study (not shown) indicated that optimal expression of Drp1 occurred at 24 h post transfection. Figure 3A shows the detection of Drp1 protein by Western blot using a polyclonal antibody against Drp1 [18]. Two endogenous Drp1 bands were detected at 79 and 75 kDa due to an alternative splicing. While the endogenous level of Drp1 in COS cell was very low without transfection (Fig. 3A), transfection with increasing amount of Drp1-cDNA (0, 6, 12, and 24 μg) resulted in similarly increased expression of the 75-kDa isoform of

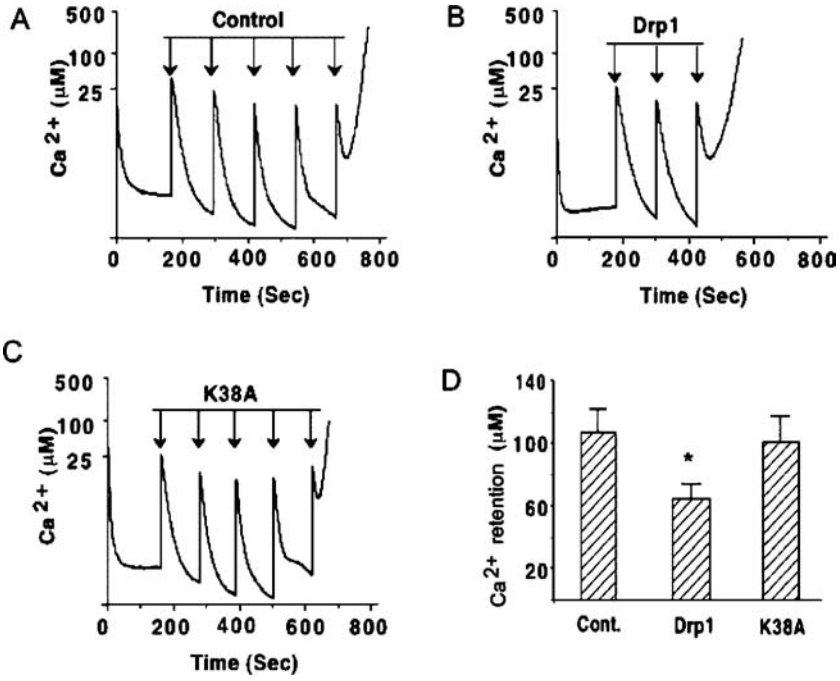

Fig. 2. Drp1 sensitizes mitochondria to calcium-induced permeability transition. (A) Ca^{2+} retention assayed as in Fig. 1 for the control COS cells (vector-transfected) showing uptake for a typical threshold of five pulses of 25 μM Ca^{2+}. (B) Transfection of Drp1 reduced the Ca^{2+} threshold to three pulses of 25 μM. (C) Expression of a dominant negative mutant Drp1(K38A) did not reduce the Ca^{2+} threshold (compare 2C with 2B). (D) Summary of four independent assays showing the significant reduction of Ca^{2+} retention in the cells expressing Drp1. All comparisons are based on the same number of cells (1×10^7) per assay. Values denote mean $\pm$ S.D. (asterisk indicates significant difference, $p < 0.05$).

Drp1 (Fig. 3A). Further increase of Drp1-cDNA to 48 μg did not lead to more expression. Examination of the GAPDH levels confirmed equal loading of the samples on the SDS gel (Fig. 3A). Parallel experiments were then carried out to assay Ca^{2+} retention in these samples. The results (Fig. 3B) indicated an inverse relationship between Ca^{2+} threshold and the Drp1 expression. The CRC was 100 μM for the control group transfected with 24 μg pcDNA3 (Fig. 3B) and non-transfected cells (Fig. 1A). Increased Drp1 expression led to a corresponding decrease of Ca^{2+} threshold (or tolerance) to 83, 67, and 58 μM (Fig. 3B). In contrast, co-transfection of Drp(K38A) (0, 12, or 24 μg DNA) together with the optimal amount of Drp1 DNA (24 μg) led to a dose-dependent increase of Ca^{2+} tolerance that corresponded to 58 ± 2, 78 ± 2, and $85 \pm 5\%$ of the non-transfected controls. Thus transfection of equal amounts of DNA encoding Drp(K38A) and Drp1 (24 μg) abolished the effect of Drp1 expression (Fig. 3C).

Mitochondrial calcium retention capacity is increased in Bcl-2 overexpressing cells

Previous studies suggested that overexpression of Bcl-2 led to increased Ca^{2+} capacity in the mitochondria of neuroblastoma cells and cardiomyocytes [6, 16]. These results have been interpreted as suggesting that by blocking MPT (i.e. protection of IMM) Bcl-2 allowed increased retention of Ca^{2+} in the mitochondria [5]. The protective effect of Bcl-2 on the IMM was also demonstrated by an increased resistance of mitochondria to undergo Ca^{2+}-induced swelling [6]. Here we have carried out the calcium retention assay in both COS cells and MCF7 cells. As expected, Fig. 4A shows that stably transfected MCF7 cell lines expressing Bcl-2 have increased Ca^{2+} threshold as compared to the controls transfected with the CMV vector. Figure 4B shows the summary from seven experiments comparing MCF7 Bcl-2 cells and control MCF7CMV cells. The Ca^{2+} threshold was 129 ± 26 μM for the CMV control group, significantly less than that for the cells expressing Bcl-2 (268 ± 65 μM, $p < 0.03$). Similarly, transient transfection of Bcl-2 in COS cells (Fig. 4C) led to an increased Ca^{2+} threshold of 200 μM as compared to 100 μM in the vector control group (COS). Thus, in contrast to Drp1, Bcl-2 confers resistance to Ca^{2+}-induced MPT in both COS cells and MCF7 cell lines (Figs. 4B and 4C).

Collaboration of Bcl-2, hFis1 and Drp1 in the regulation of Ca^{2+}-induced MPT

Since hFis1 has been shown to interact with Drp1 [23], we explored the possibility that both Drp1 and hFis1 are involved in the regulation of Ca^{2+}-induced MPT. Figures 5A and 5D

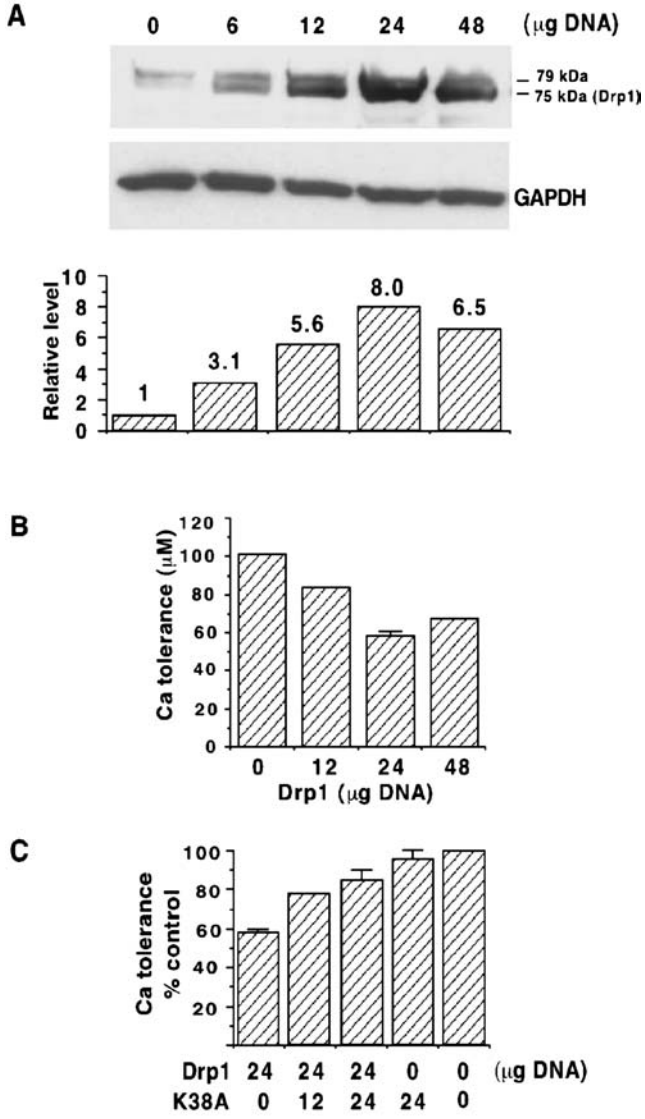

Fig. 3. Ca^{2+} retention capacity correlates inversely with Drp1 levels. (A) Western blots showing the expression of Drp1 protein (the 75-kDa band) in transfected COS cells. Transient transfection with increased amounts of pcDNA3-Drp1 DNA led to increased Drp1 levels, with maximal expression (eightfold) occurring at 24 μg of DNA. Ca^{2+} retention assay (as in Fig. 1) for permeabilized cells expressing different levels of Drp1 (B), or Drp1 and K38A (C). Results are typical of two or more independent experiments.

show that transient expression of Myc-tagged hFis1 in the MCF7Bcl-2 cells decreased the Ca^{2+} threshold for MPT. Results from six experiments (Fig. 5B) showed that expression of Myc-hFis1 (abbreviated as Fis1) significantly reduced the Ca^{2+} threshold to $69 \pm 4\%$ of the Neo control group ($p < 0.05$, $n = 6$). In contrast to the wild-type Myc-hFis1, expression of a mutant Myc-hFis1 lacking the first 31 amino acid at the N-terminal (Myc-hFis(32-152), abbreviated here as mFis1 (Fig. 5B, lane 4) was unable to reduce the Ca^{2+} threshold in MCF7Bcl-2 cells ($93 \pm 7\%$, $n = 3$). A previous morphological study [23] has shown that this particular mutant hFis1 was unable to cause mitochondrial fission. It was suggested that the first 31 amino acids of hFis1 contain crucial information for mitochondrial fission, possibly regulating Drp1 function [23]. Our results here suggest that the effect of Myc-hFis1 on mitochondrial Ca^{2+} retention may be linked to mitochondrial fission *via* Drp1. This is supported by a parallel study in the MCF7CMV cells. Figures 5C and 5D show that transient expression of Myc-hFis1 in MCF7CMV cells also led to significant decrease of Ca^{2+} threshold ($72 \pm 3\%$ of the Neo, $p < 0.05$, $n = 4$), and there was no additive effect when Drp1 and Myc-hFis1 were transfected together (data not shown). Similar to MCF7Bcl-2 cells (Fig. 5B) expression of mutant hFis1 in the MCF7CMV control cells (Figs. 5C and 5D) did not reduce the Ca^{2+} threshold ($95 \pm 7\%$ of the Neo, $n = 3$). Surprisingly, however, overexpression of Drp1 in CMV as well as Bcl-2 cells (Fig. 5D) only reduced the Ca^{2+} threshold by a small percentage and the effect was quite variable. Quantitation shows that transient transfection of Drp1 in Bcl-2 cells (Fig. 5B) had almost no effect ($93 \pm 14\%$ of the control, $n = 4$), while it only reduced the Ca^{2+} threshold to $87 \pm 10\%$ of the Neo ($n = 4$) in CMV cells (Fig. 5C). These results are unexpected because in COS cells, we observed a clear reduction of Ca^{2+} threshold upon Drp1 overexpression (Fig. 2). For further comparison, we carried out the transfection of Myc-hFis1 in COS cells. Figure 5E shows that while overexpression of Drp1 in COS cells led to decreased Ca^{2+} threshold as expected, overexpression of Myc-hFis1 had no effect compared to the Neo control. We investigated whether these differences are due to variations in endogenous levels of these three proteins. Interestingly, comparison of the Bcl-2 levels in the three types of cells (Fig. 5F) indicated an inverse correlation with the Drp1 response such that lowest Bcl-2 level in COS cells was accompanied by significant Drp1 response ($64 \pm 3\%$), intermediate Bcl-2 levels in CMV cells was associated with less Drp1 response ($87 \pm 10\%$), and finally high Bcl-2 level in MCF7Bcl-2 cells was associated with almost no response to Drp1 ($93 \pm 14\%$). While the response to Myc-hFis1 was significant in both MCF7CMV and MCF7Bcl-2 cells, there was no response to Myc-hFis1 in COS cells (Fig. 5E, lane 3). The combined studies in these cells suggest that Bcl-2, Drp1 and hFis1 collaborate in the regulation of Ca^{2+}-induced MPT.

The interactions of Drp1, hFis1, and Bcl-2

A recent structural study using NMR spectroscopy [33] has suggested that hFis1 may function as a molecular adaptor on the mitochondrial outer membrane. Although the binding of hFis1 to Drp1 has been studied [23], a competing interaction between Bcl-2 and hFis1 was not known. An interaction

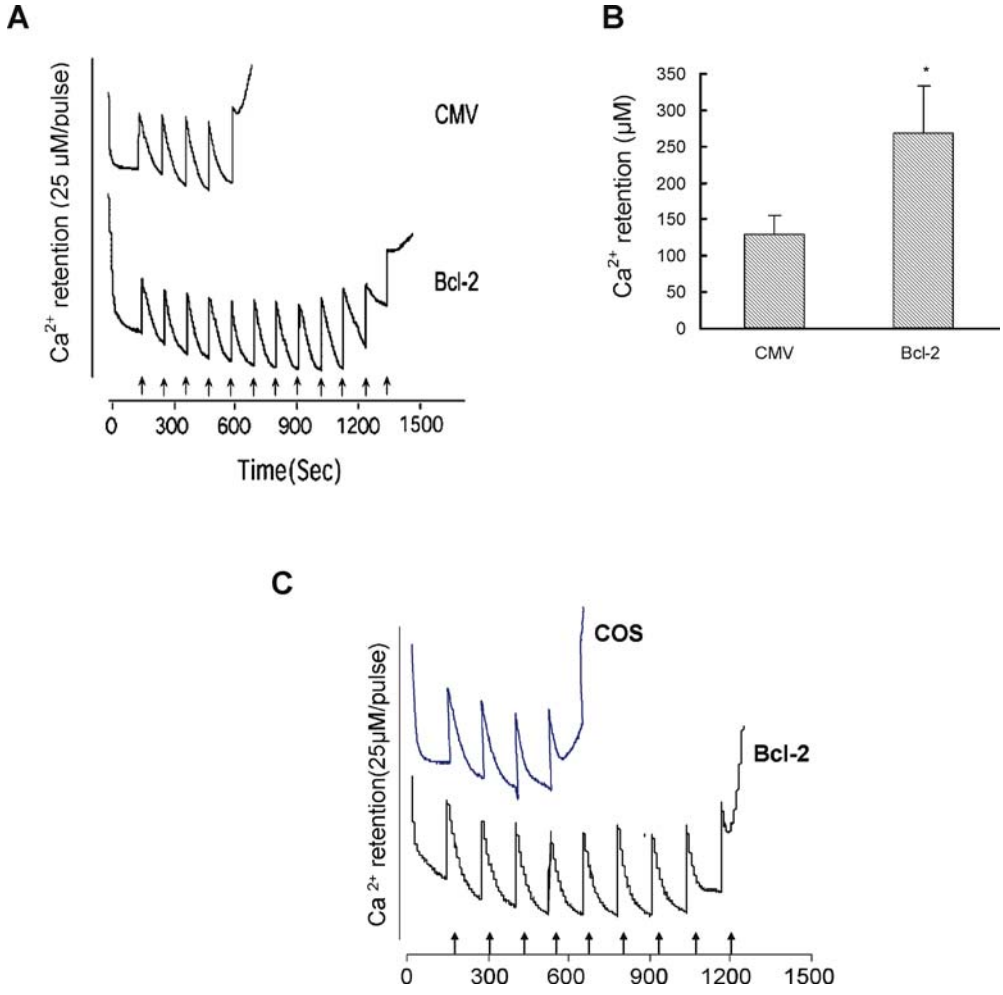

Fig. 4. Ca^{2+} retention capacity is increased in the mitochondria of Bcl-2 expressing cells. (A) MCF7 Bcl-2 expressing cells and control (CMV) cells were used directly to measure the capacity of mitochondria to retain Ca^{2+} (as in Fig. 1). (B) Summary from several experiments. (C) COS cells were transfected with plasmid encoding Bcl-2 or Neo for 24 h and used for the Ca^{2+} retention assay. Results indicate that either transient or stable expression of Bcl-2 in COS and MCF7 cells led to increased Ca^{2+} retention capacity by twofold as compared to the respective control.

between Bcl-2 and hFis1 was demonstrated here by co-immunoprecipitation experiments in MCF7 cells. We chose the MCF7Bcl-2 cells for the co-IP study because of their high expression of Bcl-2 (Fig. 6A). In MCF7Bcl-2 cells, transient transfection with Myc-hFis1 led to the expression of Myc-hFis1 in the cell lysate as shown by the Western blot with Myc antibody (Fig. 6A, lane 1). This Myc-hFis1 protein was precipitated by the Myc antibody (lane 3). In addition, Myc-hFis1 was also detected in the immune precipitate of Bcl-2 (lane 4). Comparison with the control IgG (lane 2) indicates that the immune precipitate of Bcl-2 contained much higher level of Myc-hFis1 (note the overloading of the IgG control in lane 2). Thus, the results suggest that co-immunoprecipitation of Bcl-2 and Myc-Fis1 is not due to the non-specific binding to IgG. Similarly, Bcl-2 protein was also detected in the immune precipitate of Myc (Fig. 6B, lane 3) by blotting with the Bcl-2 antibody. Note that in Fig. 6B, we have used a TrueBlot system (eBioscience) to eliminate the interference of IgG bands. Thus, Bcl-2 interaction with Myc-hFis1 was established by reciprocal immunoprecipitation experiments in MCF7Bcl-2 cells.

In addition to the interaction between hFis1 and Bcl-2, we also examined the interaction between Drp1 and Myc-hFis1 in MCF7CMV cells and MCF7Bcl-2 cells after transient expression with Myc-hFis1. Figure 6C (lane 3) shows that Drp1 antibody was able to precipitate Myc-hFis1 in the CMV cells. Again, the appearance of Myc-hFis1 in the IgG precipitate was minor and required overloading of the control IgG (lane 4). Interestingly, when MCF7 Bcl-2 cells expressing Myc-hFis1 were tested (Fig. 6D), no Myc-hFis1 protein

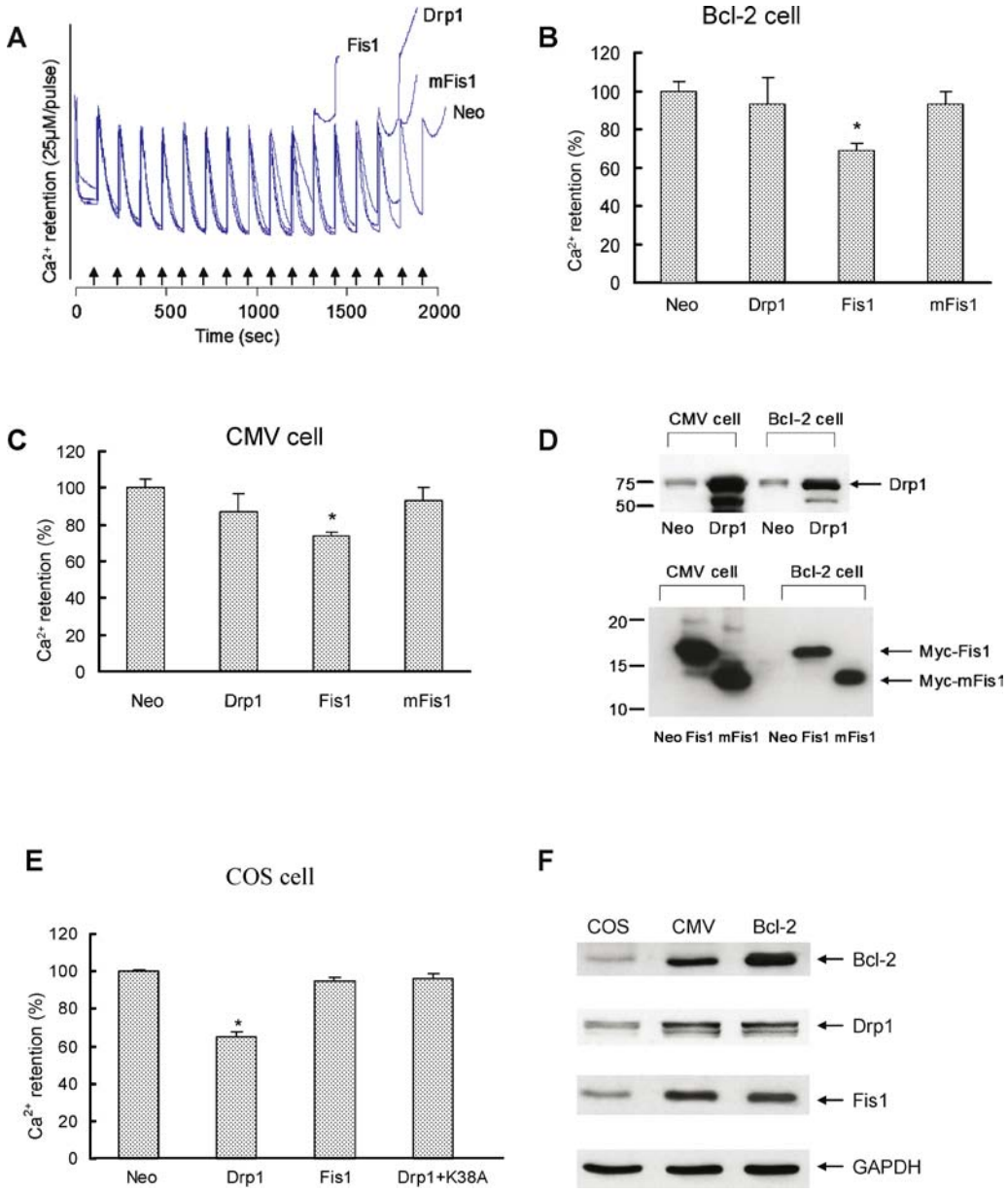

Fig. 5. Collaboration of Bcl-2, hFis1 and Drp1 in the regulation of Ca^{2+}-induced MPT. (A) MCF7 Bcl-2 cell line was transfected individually with Drp1, Myc-hFis1 (abbreviated here as Fis1), mutant Myc-hFis(32-152) abbreviated here as mFis1, and vector (Neo). After 24 h, the transfected cells were assayed for Ca^{2+} retention and compared with the Neo control. The experiments from individual assays were compiled together for the purpose of comparison. (B) Summary of four experiments showing the significantly reduced Ca^{2+} retention by Fis1 as compared to the Neo control. In contrast, mFis1 or Drp1 was unable to reduce the Ca^{2+} capacity. (C) In a parallel study, MCF7CMV cells were transfected individually with Drp1, Myc-hFis1, mutant Myc-hFis(32-152), and vector (Neo) for 24 h and then assayed for Ca^{2+} retention. (D) Western blots showing the separate detection of Drp1 (upper panel), Myc-Fis1 and Myc-mFis1 (lower panel) by anti-Drp1 or anti-Myc in the lysates of CMV and Bcl-2 cells after 24 h transfection. (E) COS cells were transfected individually with Neo, Drp1, Myc-hFis, and Drp1 + K38A for 24 h and then assayed for Ca^{2+} retention. (F) Comparison of COS, CMV, and Bcl-2 cell lysates for the endogenous levels of Bcl-2, Drp1, and hFis1. Twenty-five micrograms of cell lysates were loaded in each lane for Western analysis. The blots were first analyzed for Drp1 expression and subsequently stripped and reprobed for Bcl-2 and then hFis1. Equal loading of samples were indicated by detection of GAPDH.

was detected in the immune precipitate of Drp1 (lane 3). This difference suggests interference in the Drp1/Myc-hFis1 interaction by the high level of Bcl-2 in the MCF7Bcl-2 cells, and this interference by Bcl-2 may also explain the inability of Drp1 to reduce the Ca^{2+} threshold in the MCF7Bcl-2 cells (Fig. 5B, lane 2). However, the interference of Drp1/Myc-Fis1 interaction by proteins other than Bcl-2 cannot be excluded.

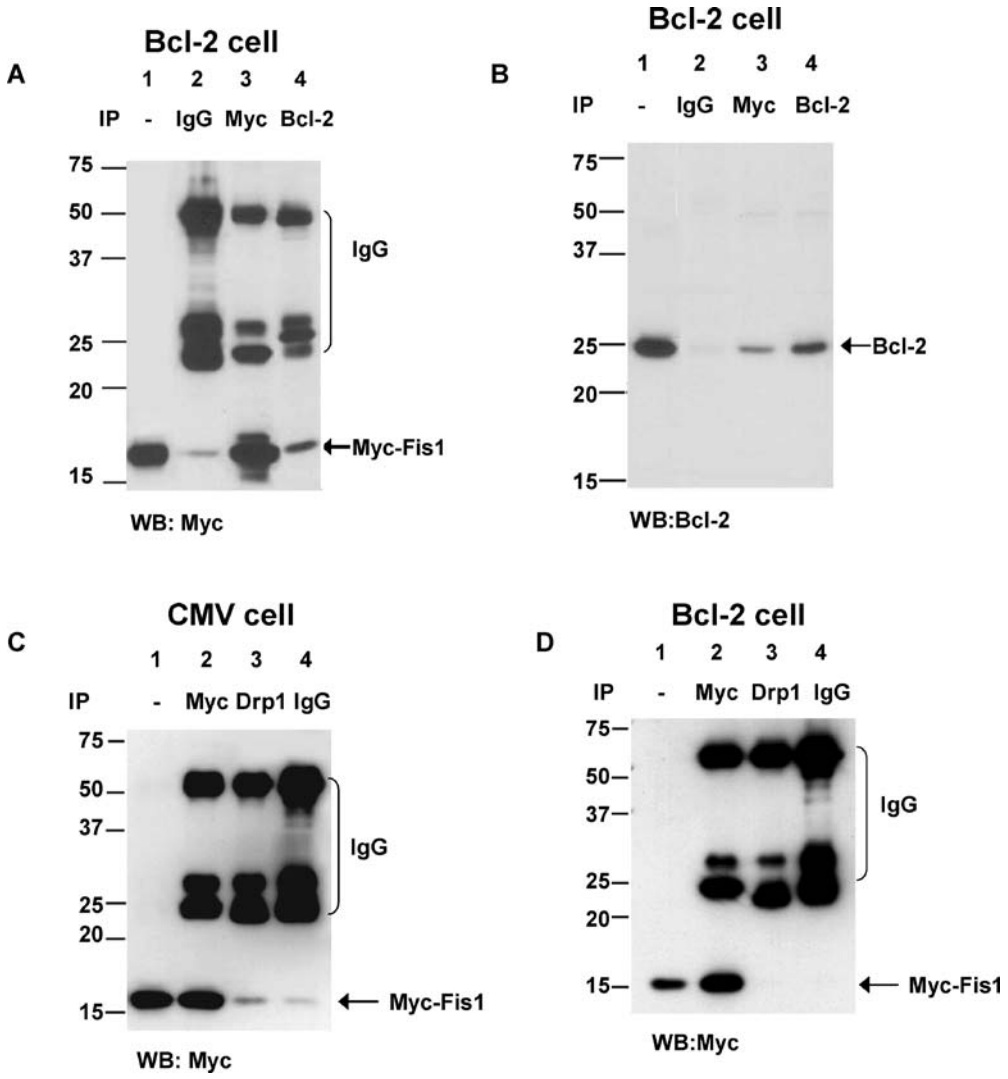

Fig. 6. The interactions of Drp1, hFis1 and Bcl-2. (A) Co-immunoprecipitation of Bcl-2 and Myc-hFis1 in MCF7Bcl-2 cells transfected with Myc-hFis1. A Western blot of the whole lysate (without immunoprecipitation) is shown in lane 1 to indicate the amounts of Myc-hFis1. Lanes 3 is the positive control to indicate the precipitation of Myc-hFis1 by the anti- Myc. Lane 4 shows that antibody to Myc can detect Myc-hFis1 in the immune precipitate of Bcl-2, and Lane 2 is the negative control to indicate a background level of Myc-hFis1 in the immune precipitate of IgG by overloading. (B) Same as (A), except the immune precipitates were detected by using antibody to Bcl-2. The results indicate that antibody to Bcl-2 can detect Bcl-2 in the immune precipitate of Myc (lane 3). In this particular experiment, a special secondary antibody named TrueBlot (eBioscience) was used to eliminate the interference by IgG. (C) Co-immunoprecipitation of Drp1 and Myc-hFis1 in MCF7CMV cells transfected with Myc-hFis1. The immune precipitate was detected with antibody to Myc. Note the detection of Myc-hFis1 (lane 3) in the immune precipitate of Drp1, while control IgG (lane 4) showed minor background after overloading the gel. (D) Failure of detection of Myc-hFis1 (lane 3) by antibody to Myc in the immune precipitate of Drp1 in MCF7Bcl-2 cells.

Antagonism between hFis1 and Bcl-2 in the regulation of mitochondrial fission and cell death

While overexpression of Drp1 has no effect on mitochondrial morphology in mammalian cells [19, 22], overexpression of hFis1 does induce mitochondrial fission [23, 24]. Here we have investigated the effect of Myc-hFis1 expression on mitochondrial morphology in MCF7 cells. Immunostaining with antibodies to the mitochondrial marker (heat shock protein 70) indicated that in MCF7CMV cells transfected with vector (Neo), the majority (91%) of the mitochondria were in a tubular network with high connectivity to each other (Fig. 7A, panel A). The population of punctate mitochondria was only 9%. Transfection of Myc-hFis1 in CMV cells for 24 h led to increases of punctate mitochondria to 40% (Fig. 7A, panel B). Double staining of the cells with both HSP70 and Myc antibody confirmed that punctate mitochondria carried the Myc marker (panel B′). This change in mitochondrial

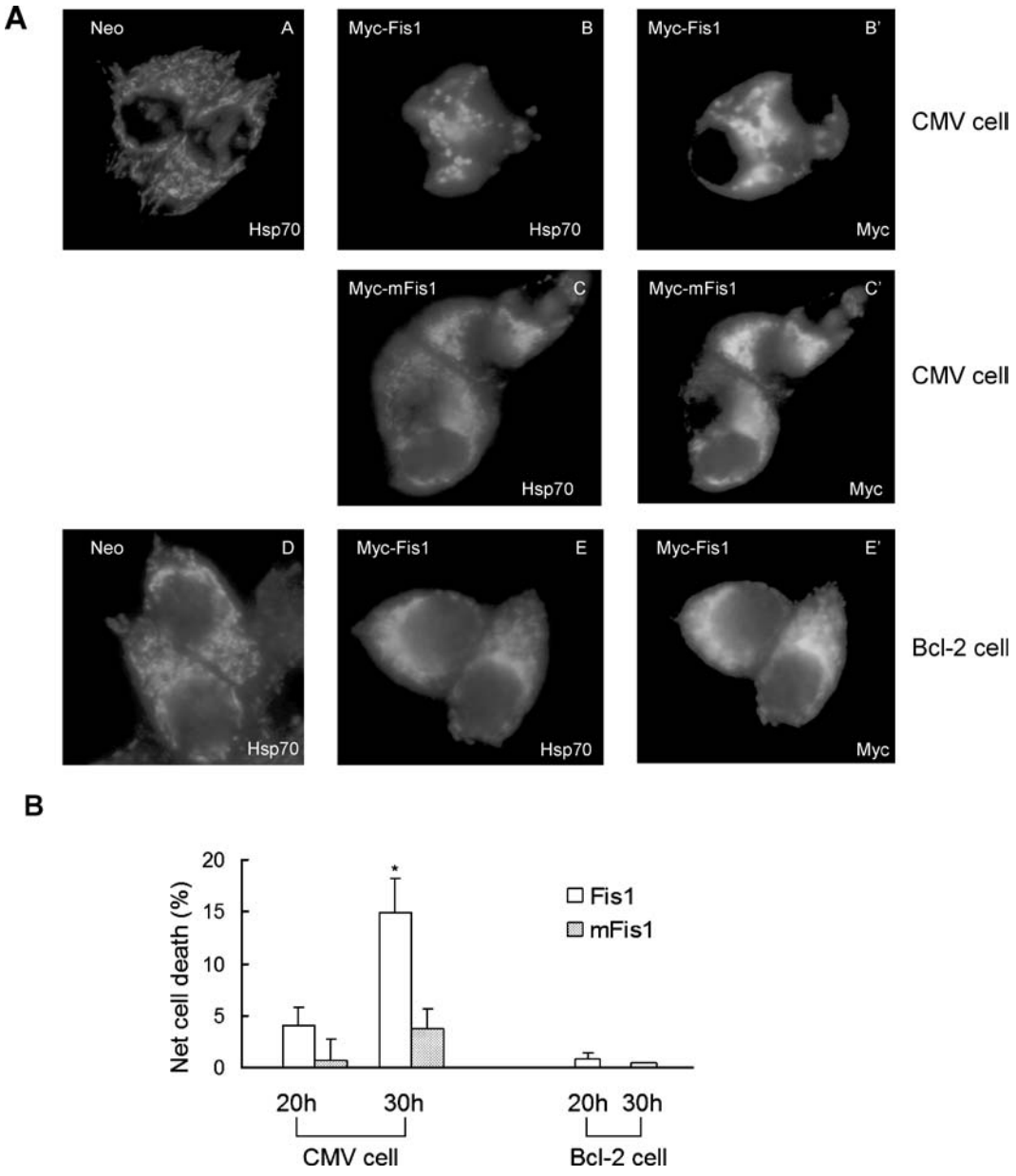

Fig. 7. Antagonism between Bcl-2 and hFis1 in the regulation of mitochondrial fission and cell death. MCF7Bcl-2 cells and MCF7CMV cells were compared for the effect of Myc-hFis1 transfection on mitochondrial morphology (A) and cell death (B). (A) To examine mitochondrial morphology, cells grown on coverslips were washed with PBS, fixed in 4% *para*-formaldehyde and stained using mouse anti-mitochondrial heat shock protein 70 (red color), and double stained with anti-Myc (green color) to ensure the cells examined were expressing Myc-hFis1. Separately, the mutant Myc-hFis1 was also transfected into the CMV cells to study the effect of mutant on mitochondrial morphology. Images were obtained using Leica DML fluorescence microscope. (B) To study Myc-hFis1-induced cell death, dead cells were stained with Trypan blue at 20 and 30 h. Net cell death was obtained after subtracting the spontaneous cell death that occurred in the control sample transfected with vector (Neo). Although not shown here, Myc-hFis1-induced cell death at 30 h (in MCF7CMV cells) was identified as apoptosis by staining with Hoechst dye. In contrast, transfection of Myc-hFis1 for 30 h was unable to induce cell death in MCF7Bcl-2 cells. Similarly, the mutant Myc-hFis1 was also unable to induce significant cell death in CMV cells.

morphology was almost completely abolished when mutant Myc-hFis (mFis1) was transfected in place of wt-Myc-hFis1 (Fig. 7A, panel C) in agreement with the previous study for clone 9 cells [23]. In contrast, expression of Myc-hFis1 in Bcl-2 cells only led to low percentage (6%) of punctate mitochondria, with most mitochondria that carried Myc marker still retained tubular morphology (Fig. 7A, panel E). After correction for the difference in transfection efficiency (30%

in Bcl-2 vs. 60% in CMV cells), the population of punctate mitochondria in the Bcl-2 cells was still threefold lower than the CMV cells. The results clearly indicate that hFis1 induces mitochondrial fission, while Bcl-2 attenuates hFis1-induced mitochondrial fission.

We also investigated the possible relationship between hFis1-induced mitochondrial fission and cell death in a time-course study (Fig. 7B). Transfection of the CMV cells or Bcl-2 cells with Myc-hFis1 for 20 h did not lead to much cell death. In the MCF7CMV cells only $4.1 \pm 1.7\%$ of cells picked up Trypan blue, while zero cell death ($0.8 \pm 0.6\%$) occurred in MCF7Bcl-2 cells. However, prolonged transfection of Myc-hFis1 (for 30 h) did induce significant population of cell death ($14.9 \pm 3.3\%$, $n = 6$, $p < 0.001$) in CMV cells, while Bcl-2 cells remained 100% viable. Unlike wild-type hFis1, mutant form of hFis1 was unable to induce cell death in CMV cells at 20 h ($0.7 \pm 1.9\%$), and at 30 h only induced $3.7 \pm 2\%$ cell death (Fig. 7B). Further study of cell death by counting apoptotic nuclei (with Hoechst dye staining, see Method section) indicated that Myc-hFis1-induced cell death in CMV cells was due to apoptotic death. After 30 h transfection with Myc-hFis1, approximately 24.4% of the CMV cells contained apoptotic nuclei (total cell number counted = 250), while no apoptotic nuclei were detected in Bcl-2 cells. The results suggest that hFis1-induced mitochondrial fission can lead to apoptosis at 30 h, and Bcl-2 inhibits hFis-1 induced apoptosis by preventing mitochondrial fission.

Discussion

We report here that overexpression of Drp1 or hFis1 sensitizes cells to Ca^{2+}-induced MPT by reducing the CRC without affecting the rate of Ca^{2+} uptake by mitochondria (see Fig. 5A, and compare the downward stroke in the Ca^{2+} pulse in different groups). In contrast, anti-death protein Bcl-2 inhibits MPT by raising the Ca^{2+} threshold. Despite the small reduction (30–40%) of the Ca^{2+} threshold by Drp1 or hFis1, this reduction is reproducible and statistically significant (Figs. 2 and 5). More importantly, we found evidence that the antagonism between Bcl-2 and Drp1 on Ca^{2+}-induced MPT is mediated by hFis1 *via* protein–protein interactions. In support of this notion, we demonstrated the interaction between hFis1 and Bcl-2 by co-immunoprecipitation experiments in MCF7Bcl-2 cells (Figs. 6A and 6B) as well as in COS cells (not shown). The normalization of the Ca^{2+} threshold by overexpressing either the mutant form of Drp1 (in COS cells) or the mutant form of hFis1 (in MCF7CMV and Bcl-2 cells) further suggests the functional relevance of the Drp1/hFis1 interaction in the regulation of Ca^{2+}-induced MPT. We have also shown that Myc-hFis1 can bind to Drp1 in MCF7CMV cells (Fig. 6C, lane 3) but not in MCF7Bcl-2 cells (Fig. 6D, lane 3). The most likely explanation for this result is that the high levels of Bcl-2 in the MCF7Bcl-2 cells compete with Drp1 for the binding to hFis1, thereby interfering with the interaction between Drp1 and hFis1. Furthermore, we have evidence that sequestration of hFis1 by Bcl-2 reduces the amounts of the free hFis1 molecule as shown by gel-filtration chromatography (Kong *et al*., unpublished results). Together, these results suggest that Bcl-2 and Drp1 binding to hFis1 are mutually exclusive. A role of hFis1 in the competitive binding of Bcl-2 versus Drp1 is also consistent with studies from other laboratories: (1) NMR structural study of hFis1 reveals a novel tetratrico-peptide repeat (TPR)-like helix bundle that suggests the protein may function as a molecular adaptor on the mitochondrial outer membrane [33]. (2) The N-terminal region of hFis1 is necessary for mitochondrial fission [23]. (3) Fluorescence resonance energy transfer and co-immunoprecipitation studies demonstrate that hFis1 interacts with Drp1 [23]. This interaction is probably weak but sufficient to allow a transient association of Drp1 with the mitochondria [23].

A recent report also indicates that overexpressed Bcl-xL was able to co-precipitate with overexpressed hFis1 in HeLa cells [24]. Based on the finding that overexpression of Bcl-xL was able to inhibit cytochrome *c* release and cell death without the prevention of mitochondrial fragmentation, it was suggested that Bcl-xL does not interfere with the fission machinery *per se* [24]. While this interpretation may be true for Bcl-xL in HeLa cells, it is certainly not the case for Bcl-2 in MCF7 cells here. By using mitochondrial marker HSP-70, we have clearly shown the inhibition of hFis1-induced mitochondrial fragmentation in the MCF7Bcl-2 cells as compared to the CMV controls (Fig. 7). The greater than threefold decrease of mitochondrial fragmentation in the Bcl-2 cells is most likely attributable to the high levels of Bcl-2 because Drp1 and hFis1 levels do not differ between MCF7Bcl-2 cells and MCF7CMV cells (Fig. 5F). A direct comparison between these two cell lines is justified as they share the same genetic background. Our results suggest that Bcl-2 can interfere with mitochondrial fragmentation directly or indirectly. The discrepancy between Bcl-2 and Bcl-xL is not clear, but is probably related to difference in protein sequence between them and warrants further investigation.

We propose that the modulation of CRC depends on a balance between the Bcl-2 expression and the activation of Drp1. Increased expression of hFis1 or Drp1 shifts the equilibrium toward the interaction between Drp1 and hFis1. By serving as the receptor for Drp1 binding, hFis1 allows the activation of Drp1 on mitochondria [23]. Subsequently, the active Drp1-GTPase may lead to the reduction of CRC *via* the severing of the OMM [22]. In contrast, increased Bcl-2 expression promotes the sequestration of hFis1, which reduces the availability of free hFis1 molecule for binding with Drp1 (Fig. 6D and Kong *et al*., unpublished data). In support of this hypothesis, in healthy cells, most Drp1 remains in the cytosol

as the inactive form [26]. However, during apoptosis, Drp1 migrates to the mitochondria and becomes activated [24, 26]. Only the active Drp1-GTPase is responsible for the reduced CRC, because the dominant negative mutant with a defective GTPase domain can abolish the effect of Drp1 and restore the high Ca^{2+} capacity (Figs. 2 and 3). Thus, hFis1 may provide a molecular platform for the competitive binding of Bcl-2 and Drp1. Mutant hFis1 that was unable to induce mitochondrial fragmentation was also unable to reduce the Ca^{2+} threshold.

The reduction of Ca^{2+} threshold by hFis1 overexpression (Fig. 5) suggests the possibility that hFis1-induced mitochondrial fission, while a normal part of the fission and fusion events in living cells, may lead to dire consequence by inadvertently triggering MPT and unwanted cell death. We have studied the relationship between hFis1-induced mitochondrial fission and cell death. Indeed, the results (Fig. 7) suggest mitochondrial fragmentation can lead to apoptotic death after prolonged expression of hFis1. Inhibition of mitochondrial fission by mutant Fis1 is accompanied by inhibition of apoptosis. The inhibition of mitochondrial fragmentation as well as cell death by Bcl-2 also supports the idea that Bcl-2 may interfere with hFis1 action. However, the lowering of Ca^{2+} threshold by hFis1 in both MCF7CMV and Bcl-2 cells suggests a separation of the Drp1/hFis1-induced sensitivity to MPT from the cell death event, i.e. the small reduction of Ca^{2+} threshold by Drp1 or hFis1 reflects a reversible state of MPT, which at early time (24 h) is not sufficient to cause cell death. It is worth mentioning that reversible opening and closing of the MPT pore is a physiological process in healthy cells [35, 14]. Since mitochondrial fission and fusion are tightly controlled processes, it is expected that the reduction of Ca^{2+} threshold by fission protein hFis1 may be opposed by fusion proteins Mfn and/or Opa1 [34, 36, 37] and this balance will maintain the integrity of the MPT pore. The fact that reduced Ca^{2+} threshold by hFis1 never exceeds 30–40% for both MCF7CMV cells and Bcl-2 cells suggest that this small reduction of CRC does not involve the irreversible opening of the pore and therefore is not detrimental to cell survival during normal fission. This is consistent with the interpretation that Drp1/hFis1 mediates mitochondrial fission *via* the severing of OMM [22], without affecting IMM. The hypothesis that fusion proteins may also participate in the regulation of Ca^{2+} threshold for MPT is also consistent with the morphological study showing the co-localization of both fission protein Drp1 and fusion protein Mfn2 at the mitochondrial fission sites [34].

We have also investigated whether Drp1 or hFis1 increased the sensitivity of cells to calcium-induced cell death. Treatment of CMV cells with calcium ionophore (A23187) for 6 h led to 24.5% of net cell death (Trypan blue assay), while the same treatment of Bcl-2 cells led to zero cell death. Although Bcl-2 can protect cells from A23187-induced death, the dominant negative Drp(K38A) does not seem to inhibit cell death caused by calcium overload (not shown). Since there is a smaller reduction of mitochondrial Ca^{2+} retention by Drp1 (30–40%) as compared with a twofold increase of Ca^{2+} retention by Bcl-2 (Figs. 2D and 4C), this may explain the lack of survival protection by the mutant Drp(K38A). This is consistent with the finding that despite the inhibitory action of Drp(K38A) on Drp1 function, it does not increase Ca^{2+} retention beyond the level of the Neo control (Fig. 3C). Our results suggest a separation of Bcl-2 mechanism from the Drp1/Fis1 effect.

In summary, we have shown the collaboration of Bcl-2, Drp1 and hFis1 in the regulation of mitochondrial CRC. While the reduction of Ca^{2+} retention by Drp1/hFis1 appears to be linked to mitochondrial fission and fusion events, the antagonist mechanism of Bcl-2 appears operated *via* inhibition of the Drp1/hFis1 interaction. The complexity of protein–protein interactions demonstrated in the present study suggest that, in addition to the previously described role of Bcl-2 in the control of apoptosis, Bcl-2 may also participate directly or indirectly in the regulation of mitochondrial fission.

Acknowledgments

We thank Dr. A.M. van der Blick for providing the Drp1 vectors and the antibody. This work was supported by National Institutes of Health (HL 39481, to THK), CIHR grant FRN 12517 (to DWA), and National Institutes of Health (DK61991 to YY). DWA holds the Canada Research Chair in Membrane Biogenesis.

References

1. Orrenius S, Nicotera P: Regulation of cell death: The calcium-apoptosis link. Nat Rev Mol Cell Biol 4: 552–565, 2003
2. Jiang S, Chow SC, Nicotera P, Orrenius S: Intracellular Ca^{2+} signals activate apoptosis in thymocytes: Studies using the Ca^{2+}-ATPase inhibitor Thapsigargin. Exp Cell Res 212: 84–92,1994
3. McGinnis KM, Gnegy ME, Wang KKW: Alterations of extracellular calcium elicit selective modes of cell death and protease activation in SH-SY5Y human neuroblastoma cells. J Neurochem 72: 1853–1863, 1999
4. Kuo TH, Kim H-RC, Zhu Lp, Yu Y, Lin HM, Tsang W: Modulation of endoplasmic reticulum calcium pump Bcl-2. Oncogene 17: 1903–1910, 1998
5. Zhu LP, Yu XD, Ling S, Brown RA, Kuo TH: Mitochondrial Ca^{2+} homeostasis in the regulation of apoptotic and necrotic cell deaths. Cell Calcium 28: 107–117, 2000
6. Zhu LP, Yu Y, Chua BHL, Ho YS, Kuo TH: Regulation of sodium–calcium exchange and mitochondrial energetics by Bcl-2 in the heart of transgenic mice. J Mol Cell Cardio 33: 2135–2144, 2001
7. Hansford RG: Physiological role of mitochondrial transport. J Bioenerg Biomembr 26: 495–508, 1994
8. Di Lisa F, Menabo R, Canton M, Barile M, Bernardi P: Opening of the mitochondriral permeability transition pore causes depletion of

mitochondrial and cytosolic NAD and is a causative event in the death of myocytes in postischemic reperfusion of the heart. J Biol Chem 276: 2571–2575, 200
9. Crompton M: Bax, Bid and the permeabilization of the mitochondrial outer membrane in apoptosis. Curr Opin Cell Biol 12: 414–419, 2000
10. Scorrano L, Ashiya M, Buttle K, Weiler S, Oakes SA., Mannella CA., Korsmeyer SJ: A distinct pathway remodels mitochondrial cristae and mobilizes cytochrome *c* during apoptosis. Dev Cell 2: 55–67, 2002
11. Kuwana T, Mackey MR, Perkins G, Ellisman MR, Latterich M, Schneiter R, Green DR, Newmeyer DD: Bid, Bax, and lipids cooperate to form supramolecular openings in the outer mitochondrial membrane. Cell 111: 331–342, 2002
12. Annis MG, Zamzami N, Zhu W, Penn LZ, Kroemer G, Leber B, Andrews DW: Endoplasmic reticulum localized Bcl-2 prevents apoptosis when redistribution of cytochrome *c* is a late event. Oncogene 20: 1939–1952, 2001
13. Green RG, Kroemer G: The pathophysiology of mitochondrial cell death. Science 305: 626–629, 2004
14. Bernardi P: Mitochondrial transport of cations: Channels, exchangers and permeability transition. Physiol Rev 79: 1127–1155, 1999
15. Murphy AN, Bredesen DE, Cortopassi G, Wang E, Fiskum G: Bcl-2 potentiates the maximal calcium uptake capacity of neural cell mitochondria. Proc Nat Acad Sci USA 93: 9893–9898, 1996
16. Zhu L, Ling S, Yu XD, Venkatesh LK, Subramanian T, Chinnadurai G, Kuo TH: Modulation of mitochondrial Ca^{2+} homeostasis by Bcl-2. J Biol Chem 274: 33267–33273, 1999
17. Bereiter-Hahn J, Voth M: Dynamics of mitochondria in living cells: Shape changes, dislocation, fusion and fission of mitochondria. Microsc Res Technol 27: 198–219, 1994
18. Smirnova E, Shurland DL, Ryazantsev SN, van der Bliek AM: A human dynamin-related protein controls the distribution of mitochodria. J Cell Biol 143: 351–358, 1998
19. Pitts KR, Yoon Y, Krueger EW, McNiven MA: The dynamin-like protein DLP1 is essential for normal distribution and morphology of the endoplasmic reticulum and mitochondria in mammalian cells. Mol Biol Cell 10: 4403–4417, 1999
20. Smirnova E, Griparic L, Shurland DL, van der Bliek, AM: Dynamin-related protein Drp1 is required for mitochondrial division in mammalian cells. Mol Biol Cell 12: 2245–2256, 2001
21. Bleazard W, McCaffery JM, King EJ, Bale S, Mozdy A, Tieu Q, Nunnari J Shaw JM: The dynamin-related GTPase Dnm1 regulates mitochondrial fission in yeast. Nat Cell Biol 1: 298–304, 1999
22. Labrousse AM, Zappaterra MD, Rube DA, van der Bliek AM: *C. elegans* dynamin-related protein DRP-1 controls severing of the mitochondrial outer membrane. Mol Cell 4: 815–826, 1999
23. Yoon Y, Krueger EW, Oswald BJ, McNiven MA: The mitochondrial protein hFis1 regulates mitochondrial fission in mammalian cells through an interaction with the dynamin-like protein DLP1. Mol Cell Biol 15: 5409–5420, 2003
24. James DI, Parone PA, Mattenberger Y, Martinou JC: hFis1, a novel component of the mammalian mitochondrial fission machinery. J Biol Chem 278: 36373–36379, 2003
25. Stojanovski D, Koutsopoulos OS, Okamoto K Ryan MT: Levels of human Fis1 at the mitochondrial outer membrane regulate mitochondrial morphology. J. Cell Sci. 117: 1201–1210, 2004
26. Frank S, Gaume B, Bergmann-Leitner ES, Leitner WW, Robert EG, Catez F, Smith CL, Youle RL: The role of dynamin-related protein 1, a mediator of mitochondrial fission, in apoptosis. Dev Cell 1: 515–525, 2001
27. Frieden M, James D, Castelbou C, Danckaert A, Martinou JC, Demaurex N: Ca^{2+} homeostasis during mitochondrial fragmentation and perinucear clustering induced by hFis1. J Biol Chem 279: 22704–22714, 2004
28. Zhu W, Leber B, Andrews DW: Cytoplasmic *O*-glycosylation prevents cell surface transport of E-cadherin during apoptosis. EMBO J 20: 5999–6007, 2001
29. Moreadith RW, Fiskum G: Isolation of mitochondria from ascites tumor cells permeabilized with digitonin. Anal Biochem 137: 360–367, 1984
30. Evetodienko YV, Teplova VV, Azarashvily TS, Kudin A, Prusakova O, Virtanen I, Saris NEL: The Ca^{2+} threshold for the mitochondrial permeability transition and the content of proteins related to Bcl-2 in rat liver and Zajdela hepatoma mitochondria. Mol Cell Biochem 194: 251–256, 1999
31. Liu BF, Xu X, Fridman R, Muallem S, Kuo TH: Consequence of functional expression of the plasma membrane Ca^{2+} pump isoform 1a. J Biol Chem 271: 5536–5544, 1996
32. Zhu W, Cowie A, Wasfy GW, Penn LZ, Leber B, Andrews DW: Bcl-2 mutants with restricted subcellular location reveal spatially distinct pathways for apoptosis in different cell types. EMBO J 15: 4130–4141, 1996
33. Suzuki M, Jeong SY, Karbowski M, Youle RJ, Tjandra N: The solution structure of human mitochondria fission protein Fis1 reveals a novel TPR-like helix bundle. J Mol Biol 334: 445–458, 2003
34. Karbowski M, Lee YJ, Gaume B, Jeong SY, Frank S, Nechushtan A, Santel A, Fuller M. Smith CL, Youle RJ: Spatial and temporal association of Bax with mitochondrial fission sites, Drp1, and Mfn2 during apoptosis. J Cell Biol 159: 931–938, 2002
35. Ichas F, Jouaville LS, Mazat JP: Mitochondria are excitable organelles capable of generating and conveying electrical and calcium signals. Cell 89: 1145–1153, 1997
36. Legros F, Lombes A, Frachon P, Rojo M; Mitochondrial fusion in human cells is efficient, requires the inner membrane potential, and is mediated by mitofusins. Mol Biol Cell 13: 4343–4354, 2002
37. Lee YJ, Jeong SY, Karbowski M, Smith CL, Youle RJ: Roles of the mammalian mitochondrial fission and fusion mediators Fis1, Drp1, and Opa1 in apoptosis. Mol Biol Cell 15: 5001–5011, 2004